

Figure captions

Fig. 1. Pairwise competitive interactions in a phyllosphere *Pseudomonas* spp. community. Rows reflect strains in the resident state, while columns reflect strains in the invader state. Dashed red lines through interaction matrix denote within-between clade divisions for ease of visualization. Phylogeny modified from Humphrey *et al.* (2014).

Fig. 2. Phylogenetic distribution of life history trait variation within a *Pseudomonas* spp. community. **a.** Life history components are maximum growth rate (r_m), lag phase (l), maximum yield (K), derived from individual microcosm growth experiments; and components of offensive (C_o), defensive (C_d), overall (C_w) competitiveness, resistance to toxicity (C_r), toxicity (C_t), and overall interference capacity (I_w) derived from a pairwise competitive interaction network (see *Methods*). Column z-score of each trait value indicated by color. **b.** Smoothed frequency distributions of trait values for each measured trait by clade (*P. fluorescens* and *P. syringae*). **c.** Pairwise correlations and principle component analysis (PCA) (**d**) of nine traits revealed clear dissimilarities in trait distributions and patterns of co-variance between clades. Correlations with text values reflect magnitude of each Pearson's ρ where the FDR corrected $p < 0.05$; comparisons with FDR-corrected $p < 0.10$ are italicized. **d.** PCA 95% envelopes per clade depicted as solid or dashed ellipses. Dots are labeled with strain IDs. Individual trait vector loadings are in blue for resource use traits and orange for competitive indexes).

Fig. 3. Prevalence of intransitive interactions in a *Pseudomonas* spp. interaction network. **a.** Types of interaction trios resulting in facilitation or rock-paper-scissors (R-P-S) competitive asymmetries. N = number of trios meeting the given criteria out of the total trios analyzed (see *Methods*). **b.** Frequency distributions of how often each strain played the facilitator (A), the knocked-out intermediate (B), or the facilitated (C). Several strains

played multiple roles; strains in facilitative trios with as well as without toxic intermediates are indicated with black triangles to the left of the strain IDs. Panel (b) inset displays the distribution of the number of unique strains that played each combination of roles. Only 06B played all three roles. The probability of playing *A*, *B*, or *C* roles in facilitative trios varied with (c) overall competitiveness, C_w , as well as (d) resistance. e. ΔC_w plotted against baseline C_w shows initially weaker *P. syringae* strains benefit the most from indirect interactions (Pearson's $\rho = -0.67$), while *P. fluorescens* fitness remains relatively unaffected by indirect interactions ($\rho = 0.74$). f. Net competitive fitness ($C'_w = C_w + \Delta C_w$) after considering indirect effects weakens competitive hierarchies among *P. syringae* ($\rho = 0.50$) but has little effect on *P. fluorescens* competitive fitness ($\rho = 0.98$).

Figures

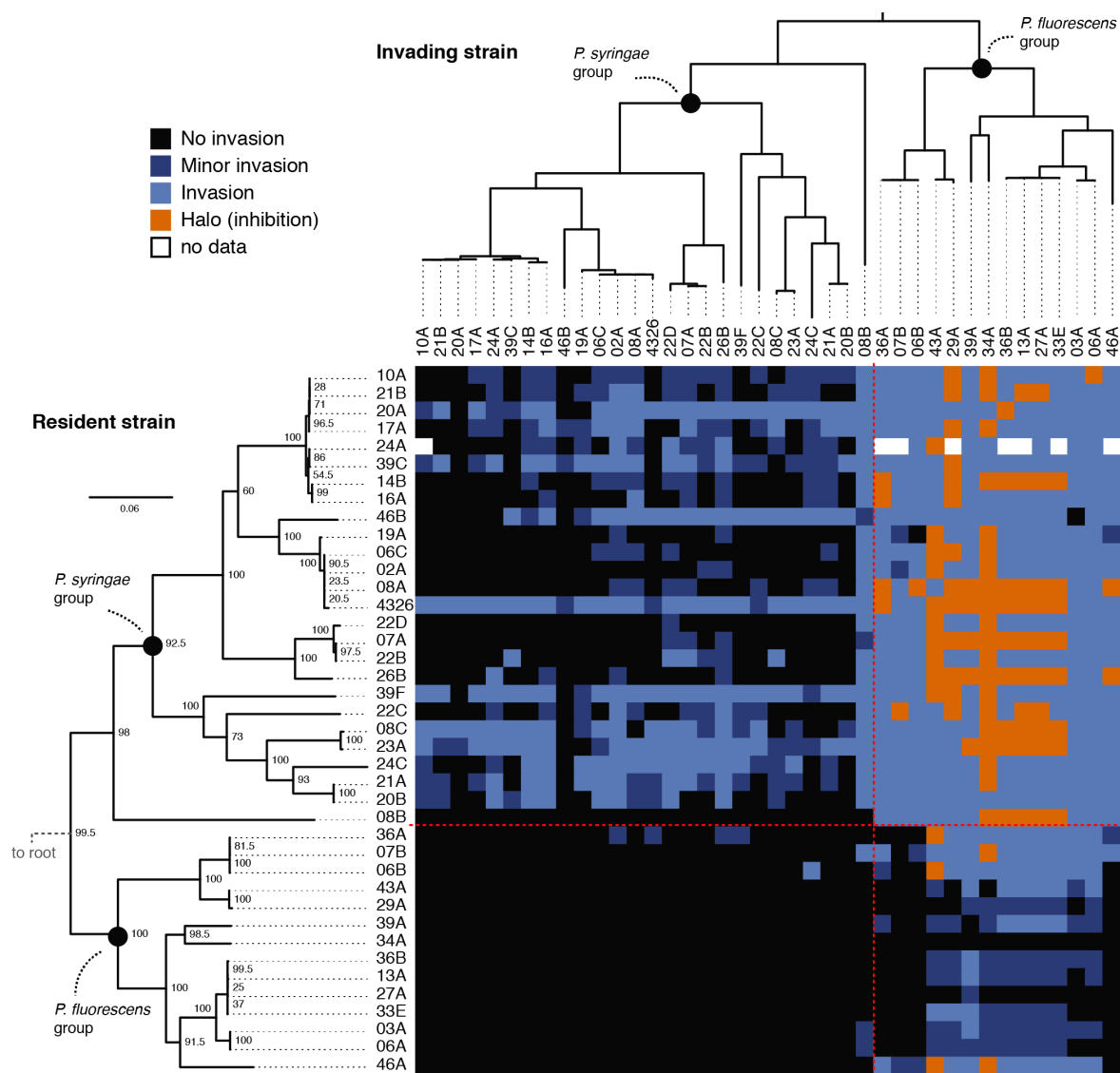


Figure 1:

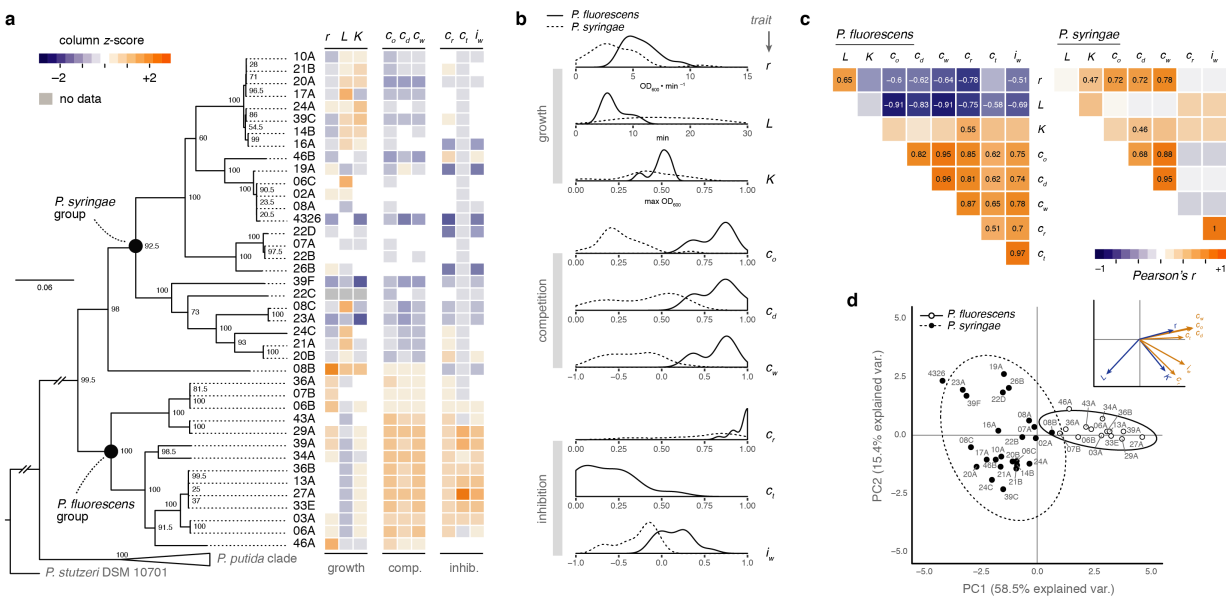


Figure 2:

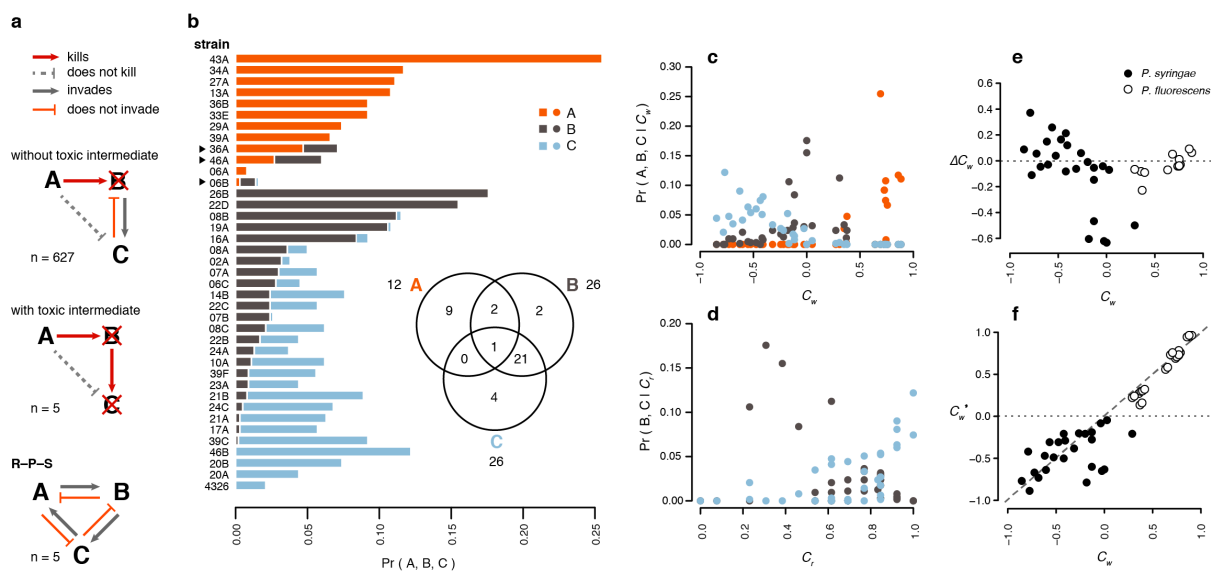


Figure 3: